Article

Not peer-reviewed version

Ligand-Independent Vitamin D Receptor Actions Essential for Keratinocyte Homeostasis in the Skin

Satoko Kise *, Shinichi Morita, Toshiyuki Sakaki *, Hiroyukli Kimura, Seigo Kinuya, Kaori Yasuda *

Posted Date: 18 November 2024

doi: 10.20944/preprints202411.1167.v1

Keywords: vitamin D receptor; keratinocyte homeostasis; ligand-independent VDR action; hyperkeratosis; alopecia

 doi:10.20944/preprints202411.1167.v1

Article

Ligand-Independent Vitamin D Receptor Actions Essential for Keratinocyte Homeostasis in the Skin

Satoko Kise [1,2,3,*], Shinichi Morita [4,5], Toshiyuki Sakaki [3,*], Hiroyuki Kimura [1], Seigo Kinuya [1], Kaori Yasuda [3,*]

[1] Department of Nuclear Medicine, Kanazawa University Hospital, Kanazawa University, 13-1 Takara-machi, Kanazawa, Ishikawa, 920-8641, Japan
[2] Division of Probe Chemistry for Disease Analysis, Research Center for Experimental Modeling of Human Disease Kanazawa University, 13-1 Takara-machi, Kanazawa, Ishikawa 920-8460, Japan
[3] Department of Pharmaceutical Engineering, Faculty of Engineering, Toyama Prefectural University, 5180 Kurokawa, Imizu, Toyama 939-0398, Japan
[4] Division of Evolutionary Developmental Biology, National Institute for Basic Biology, 38 Nishigonaka, Myodaiji, Okazaki 444-8585, Japan
[5] Department of Basic Biology, School of Life Science, The Graduate University for Advanced Studies, SOKENDAI, Hayama, Miura 240-0115, Japan
* Correspondence: skise1998@stu.kanazawa-u.ac.jp (S.Kise); tsakaki@pu-toyama.ac.jp (T.S); kyasuda@pu-toyama.ac.jp (K.Y)

Abstract: Recently, we demonstrated that the alopecia observed in vitamin D receptor gene deficient (VDR-KO) rats is not seen in rats with a mutant VDR (R270L/H301Q), which lacks ligand-binding ability, suggesting that the ligand-independent action of VDR plays a crucial role in maintaining the hair cycle. Since VDR-KO rats also showed abnormalities in the skin, the relationship between alopecia and skin abnormalities was examined. To clarify the mechanism of actions of vitamin D and VDR in the skin, protein composition, and gene expression patterns in the skin were compared among VDR-KO, VDR (R270L/H301Q), and wild-type (WT) rats. While R270L/H301Q rats exhibited normal skin formation similarly to WT rats, VDR-KO rats showed a remarkable hyperkeratosis and trans-epidermal water loss in the skin. RNA sequencing and proteomic analysis revealed that the gene and protein expression patterns in VDR-KO rats significantly differed from those in WT and VDR (R270L/H301Q) rats, with a marked decrease in the expression of factors involved in Shh, Wnt, and Bmp signaling pathways, a dramatic reduction in the expression of hair keratins, and a substantial increase in the expression of epidermal keratins. This study clearly demonstrated that non-liganded VDR is significantly involved in the differentiation, proliferation, and cell death of keratinocytes in hair follicles and the epidermis.

Keywords: vitamin D receptor; keratinocyte homeostasis; ligand-independent VDR action; hyperkeratosis; alopecia

1. Introduction

Vitamin D is a multifunctional hormone and is usually obtained from foods like fish or synthesized in the skin when 7-dehydrocholesterol is cleaved by UV light, followed by isomerization in the body, to produce vitamin D3 (VD3). VD3 is initially hydroxylated in the liver by P450 enzymes such as CYP2R1 and CYP27A1 to form 25-hydroxyvitamin D3 (25D3), which is referred to as pro-vitamin D3. Then, 25D3 is converted to 1α,25-dihydroxyvitamin D3 (1,25D3), the active form of vitamin D3, by CYP27B1 in the kidneys. 1,25D3 binds to the vitamin D receptor (VDR) present in the cytoplasm, inducing VDR's translocation to the nucleus. Subsequently, VDR forms a heterodimer with the retinoid X receptor (RXR), binds to vitamin D response elements (VDREs), and regulates the expression of genes involved in bone formation and calcium homeostasis (such as calcium channels, osteocalcin, and osteopontin). This mechanism is widely known as the classical genomic action of vitamin D [1] (Figure 1).

 doi:10.20944/preprints202411.1167.v1

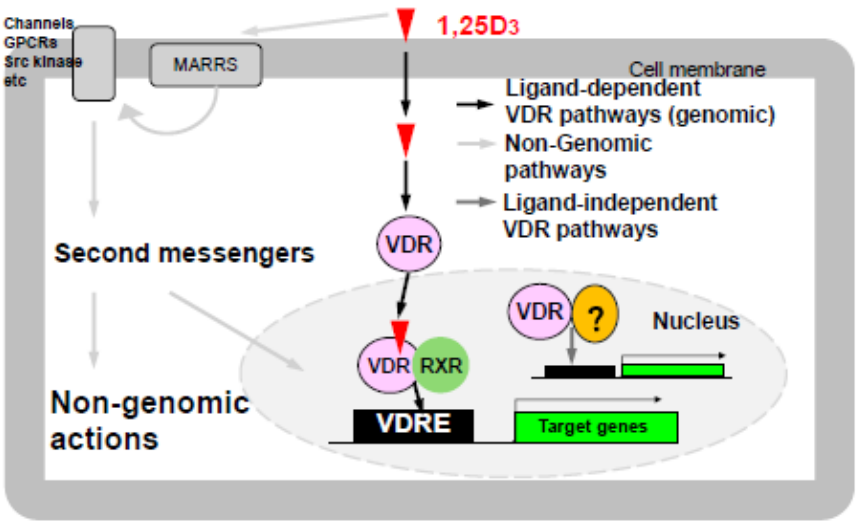

Figure 1. Multiple mechanisms of Active Vitamin D and VDR Actions.

MARRS: An abbreviation for membrane-associated rapid response sterol binding, which is identical to ERp57. The question marks indicate a protein factor that forms complexes with non-liganded VDR, with Hairless being one known example.

On the other hand, recent studies have highlighted the importance of non-genomic actions of vitamin D (Figure 1) [2–4] and ligand-independent VDR functions [5,6]. Rats with Cyp27b1 gene deficiency (CYP27B1-KO) exhibit much more significant decreases in serum calcium levels and growth inhibition compared to rats with vitamin D receptor gene deficiencies (VDR-KO) [7]. This is thought to be based on the loss of non-genomic actions of 1,25D3 that are not mediated by VDR. Additionally, type II rickets caused by mutations in the VDR gene often leads to alopecia. Mutations in the DNA-binding domain or RXR interaction site of VDR cause alopecia, whereas mutations in the ligand-binding domain do not. This suggests that ligand-dependent VDR action, i.e., the canonical genomic action of vitamin D, is not essential for the hair cycle.

To evaluate how vitamin D acts in various organs and cell types, we generated genetically modified rats (GM rats) with altered vitamin D-related genes. CYP27b1-KO rats cannot produce 1,25D3, while VDR-KO rats lack most of the ligand-binding domain of VDR [7,8]. Furthermore, we produced rats with mutant VDRs. VDR's Arg270 forms a hydrogen bond with the 1α-hydroxyl group of 1,25D3, and His301 forms a hydrogen bond with the 25-hydroxyl group. Therefore, the VDR-R270L mutant, where Arg270 is replaced with Leu, has an affinity for 1,25D3 reduced to about 0.1% that of WT, and the VDR-H301Q mutant, where His301 is replaced with Gln, has an affinity for both 1,25D3 and 25D3 reduced to several tens of that of WT. Humans with corresponding VDR-R274L or VDR-H301Q mutations exhibit type II rickets without alopecia.

We also created rats having the double mutant VDR-R270L/H301Q, which has almost no ability to bind both 1,25D3 (less than 0.01% of that of VDR-WT) and 25D3 (less than 1% of VDR-WT). The VDR-R270L/H301Q rats appear to be the best animal model for analyzing the function of ligand-independent VDR [6,8]. As shown in Figure 2, comparing WT rats with VDR-R270L/H301Q rats highlights the effects of ligand-dependent VDR. Additionally, comparing VDR-R270L/H301Q rats with VDR-KO rats reveals the effects of ligand-independent VDR. Since only VDR-KO rats exhibit alopecia with age, this indicates that ligand-independent VDR action plays a crucial role in the hair cycle. On the other hand, bone formation abnormalities are observed in both VDR-R270L/H301Q and VDR-KO rats, suggesting that ligand-dependent VDR action is important for bone formation.

 doi:10.20944/preprints202411.1167.v1

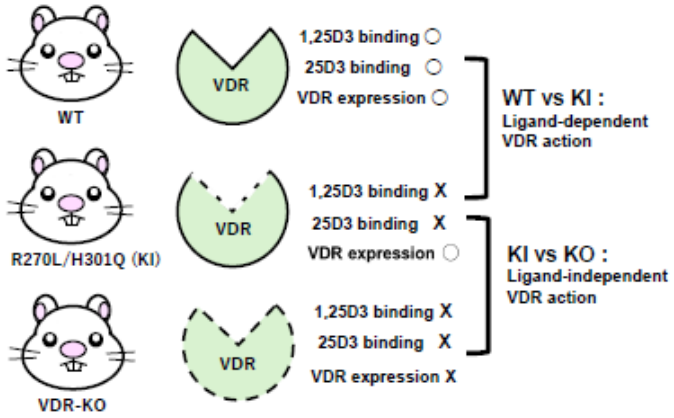

Figure 2. The three types of rats used in this study. WT: Wild-type rats, KI: Rats expressing mutant VDR (R270L/H301Q), KO: VDR gene-deficient rats. The 1,25D3 and 25D3 cannot bind to VDR (R270L/H301Q). The expression level of VDR (R270L/H301Q) in KI rats is nearly the same as that of normal VDR in WT rats. By comparing WT and KI rats, ligand-dependent actions of VDR can be highlighted, and by comparing KI and KO, the functions of non-liganded VDR can be delineated.

Vitamin D contributes to hair growth during the anagen phase of the hair cycle by activating the Wnt signaling pathway and is involved in maintaining skin homeostasis, wound healing [9]. Keratinocyte-specific VDR gene-deficient KO mice, generated by crossing mice expressing Cre recombinase under the control of the Krt14 promoter with mice carrying loxP sites flanking the VDR gene, exhibit alopecia and impaired wound healing [9]. From these results, it was hypothesized that VDR is necessary for wound healing, though more so for keratinocyte migration rather than proliferation [10]. On the other hand, Tian et al. [11] found that the administration of 1,25D3 was effective for wound repair, suggesting a ligand-dependent VDR action. Calcium and 1,25D3 were thought to be necessary for keratinocyte differentiation and cornified envelope formation [12]. While the involvement of CaSR, PLC, PKC, and AP-1 factors has been suggested, the involvement of VDR remains unclear. Thus, how VDR is involved in keratinocyte proliferation and migration is not yet fully understood. Recently, Joko et al. [13] suggested that VDR plays a crucial role in inducing keratinocyte apoptosis during the catagen phase of the hair cycle. They showed the presence of "surviving epithelial strands'' in the hair follicles of VDR-KO mice, which results in dermal cyst accumulation. In this study, to clarify whether the skin abnormalities in VDR-KO rats that follow alopecia are related to the dermal cyst formation or arise through completely different mechanisms, we attempted to elucidate the function of VDR in maintaining skin homeostasis by evaluating differences in skin phenotypes, functions, gene expression, and protein expression among WT, VDR-R270L/H301Q (hereafter simply referred as KI), and VDR-KO (KO) rats.

2. Results

2.1. Comparison of Skin Morphology from Young Stage to Older Stage Among WT, KI, and KO Rats with HE Staining

The skin morphology of WT, KI, and KO rats was analyzed across different developmental stages. At the young stage (4 weeks), no discernible differences were observed among the three groups. However, by the middle stage (7 weeks) and older stage (22 weeks), significant skin abnormalities, including cyst formation and hyperkeratosis, were evident exclusively in KO rats (Figure 3). These findings indicate that ligand-independent VDR functions play a crucial role not only in maintaining the hair cycle but also in preserving skin structure and function.

 doi:10.20944/preprints202411.1167.v1

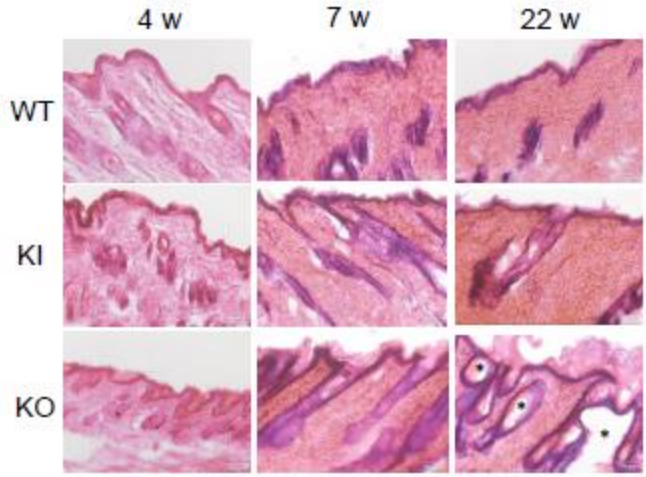

Figure 3. H&E-staining of dorsal skin of KI and KO rats at 4, 7, and 22-weeks of age.

2.2. VDR Localization in the Rat Skin via Immunofluorescence Analysis

VDR is known to be expressed in keratinocytes and in the lower proximal region of hair follicles. To assess the localization of KI in the skin of KI rats, immunofluorescence analysis was conducted on skin samples from 7-week-old rats. Similarly to WT and KI rats exhibited the VDR expression in keratinocytes and the lower proximal cup of the hair follicle. In contrast, no VDR signal was detected in the skin of KO rats(Figure 4).

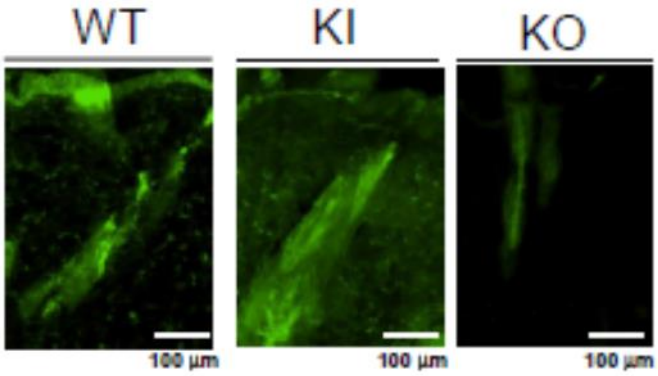

Figure 4. Immunostaining analysis of VDR in dorsal skin of WT, KI, and KO rats.

2.3. SDS-PAGE Analysis of Rat Skin Proteins with CBB Staining, and Western Blot Analysis Using Anti-Krt14 and Anti-Pan-Keratin Antibodies

To evaluate the overall protein composition in the skin of each rat, SDS-PAGE followed by CBB staining was performed on skin samples from 4-, 15-, and 30-week-old rats. At the young stage (4 weeks), no significant differences were observed among the three groups (Figure 5). However, by the middle stage (15 weeks) and older stage (30 weeks), the protein pattern in KO rats showed marked differences compared to both WT and KI rats, with a notable disparity around the 55 kDa region. Given the hyperkeratosis observed in VDR-KO rats through HE staining, we conducted Western blotting using the antibody against the keratin marker Krt14, and anti-pan-keratin antibody (PCK26), which detects rat keratin 1 (66 kDa), keratin 5 (58 kDa), and keratin 8 (52 kDa). Consistent with expectations, KO rats exhibited a significant overexpression of these keratin markers (Suppl. Figure 2).

 doi:10.20944/preprints202411.1167.v1

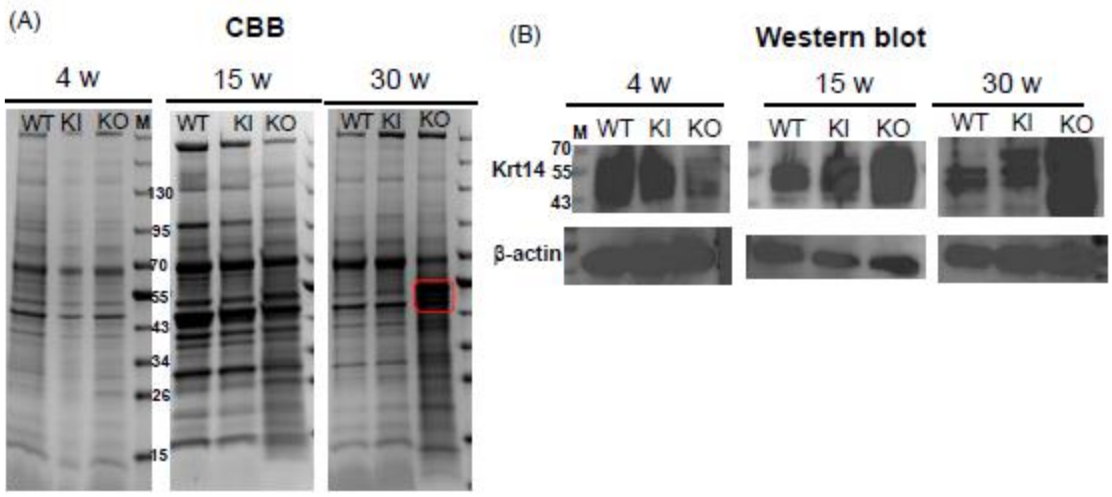

Figure 5. SDS-PAGE (A) and Western blot analysis of Krt14 (B) in dorsal skin protein prepared from WT, KI, and KO rats at 4, 15, and 30 weeks of age. M: Thermo Scientific PageRuler Prestained NIR Protein Ladder.

2.4. Trans Epidermal Water Loss (TEWL) in the Rat Skin

TEWL refers to the passive evaporation of water from the skin into the external environment. It serves as a valuable indicator for assessing skin health, hydration levels, and is commonly used to evaluate skin disease models [14]. Typically, low TEWL values reflect a healthy and intact skin barrier, whereas elevated TEWL values suggest a compromised barrier function. Across all stages examined (5, 10, and 30 weeks), VDR-KO rats consistently exhibited higher TEWL values compared to the other groups, indicating impaired skin barrier integrity (Figure 6)

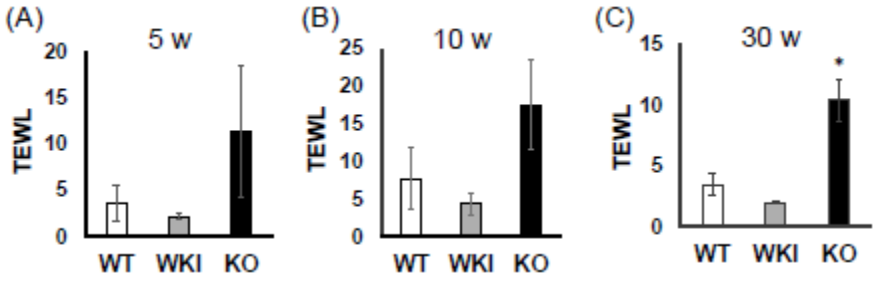

Figure 6. Comparison of trans-epidermal water loss in the skin of WT, KI, and KO rats at 5, 10, and 30 weeks of age.

2.5. Gene Expression Analysis by Bulk RNA-Seq

The symptoms of hair loss, skin thickening, and cyst formation were observed exclusively in KO rats and not in WT or KI rats (Figure 3, and Suppl. Figure 1). Additionally, Trans epidermal water loss (TEWL) was significantly higher only in KO rats, suggesting a decline in skin barrier function (Figure 6). Furthermore, in 30-week-old KO rats, remarkable expression of the epidermal keratin, Krt14, was observed (Figure 5). These results suggest that the gene expression profile in KO rats differs significantly compared to WT and KI rats. Thus, we analyzed 9 RNA-seq libraries created from skin tissues of three groups (WT, KO and KI groups, with 3 rats in each group). We quantified the gene expression levels and performed hierarchical clustering analysis on the 9 samples. As a result, samples within each group clustered together, with each group exhibiting a distinct gene expression pattern (Figure 7 A).

 doi:10.20944/preprints202411.1167.v1

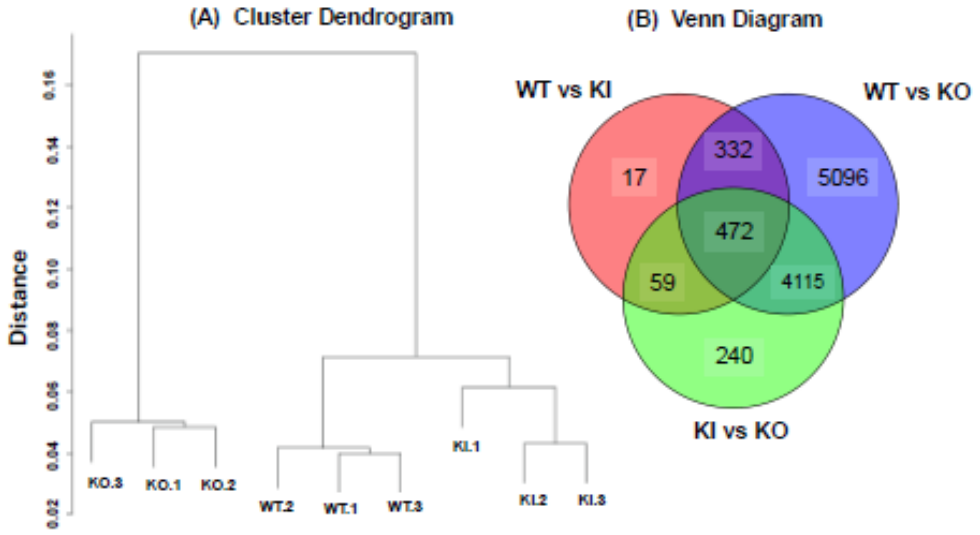

Figure 7. Cluster diagram of WT, KI, and KO rats (A), and Venn diagram among WT vs KO, WT vs KI, and KI vs KO (B).

We then performed two different types of comparisons to identify transcripts involved in keratinocyte homeostasis under the regulation of VDR (FDR < 0.05). First, we compared the WT and KO groups to comprehensively identify genes regulated by VDR in both ligand-dependent and ligand-independent manners. This analysis identified 10,015 DEGs (Figure 7B). Subsequently, to identify genes regulated by VDR in ligand-dependent manner, we compared the WT and KI groups (Figure 2). This comparison identified 880 DEGs. Many of the 880 DEGs overlapped with those obtained in the WT vs KO comparison, indicating the accuracy of this analysis (Figure 7 B). In addition, the KI vs. KO comparison, which highlights ligand-independent VDR action (Figure 2), revealed 4,886 DEGs. It is also noteworthy that the number of DEGs identified in the WT vs. KI comparison was significantly smaller than that in the KI vs. KO comparison. These findings suggest that most genes regulated by VDR in the skin are likely controlled by non-liganded VDR.

Figure 8 compares the expression of the Shh pathway (Shh), Wnt signaling pathway (Cttnb1 [β-catenin], Lef1, Wnt10b, Wise), and BMP pathway (Bmp4, Noggin). The results indicate a pronounced decrease in gene expression in KO rats compared to WT and KI rats, with the exception of Wise, known as an inhibitor of both the Wnt and Bmp signaling pathways [15]. This suggests that the Wnt signaling pathway is significantly suppressed in KO rats relative to WT and KI rats. The Bmp pathway inhibitor Noggin is also reduced in KO rats. However, considering the collective influence of Bmp4, Noggin, and Wise, it can be deduced that the progression of the Bmp pathway is likewise hindered in KO rats. These pathways are essential for sustaining the hair cycle [16], and the observed inability of KO rats to maintain this cycle further supports this conclusion. As depicted in Figure 8, the gene expression levels in KI rats closely resembled those in WT rats, consistent with the normal hair cycle maintenance observed in KI rats (Suppl. Table S1).

Preprints.org (www.preprints.org) | NOT PEER-REVIEWED | Posted: 18 November 2024 doi:10.20944/preprints202411.1167.v1

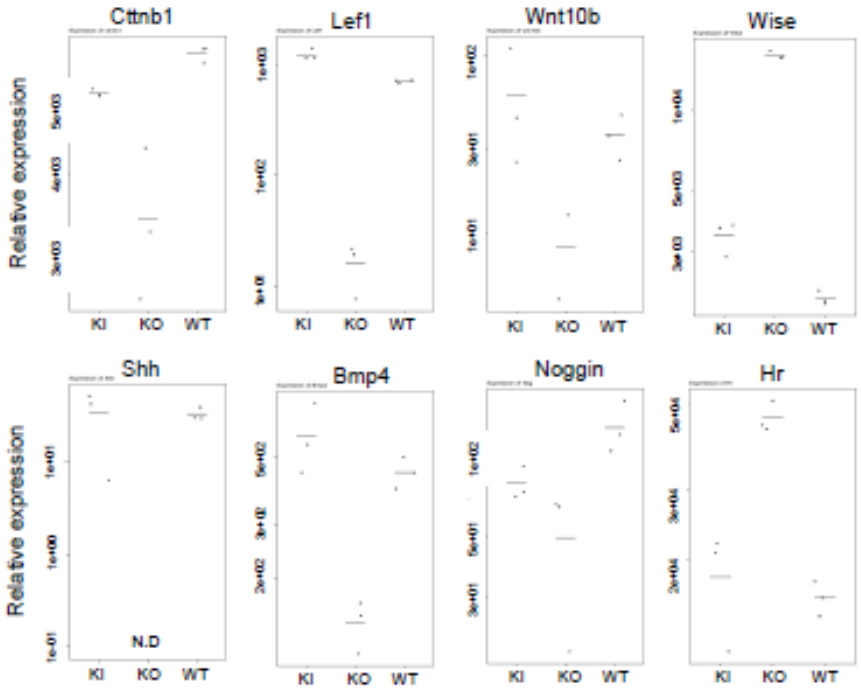

Figure 8. Comparison of mRNA levels of genes required for hair follicle development and regeneration among WT, KO, and KI rats.

Figure 9 highlights keratins that were significantly increased only in KO (Suppl. Table S2). These keratins are all known as epidermal keratins and are located in the epidermis. The epidermis consists of the basal, spinous, granular, and cornified layers. Krt5 and 14 are mainly expressed in the basal layer, while Krt1 and 10 are expressed in the spinous, granular, and cornified layers. After hair loss, the disappearance of hair follicle keratinocytes and differentiation into epidermal keratinocytes, as well as cyst formation and skin thickening due to proliferation, led to the formation of significantly different skin in 30-week-old KO rats compared to WT and KI.

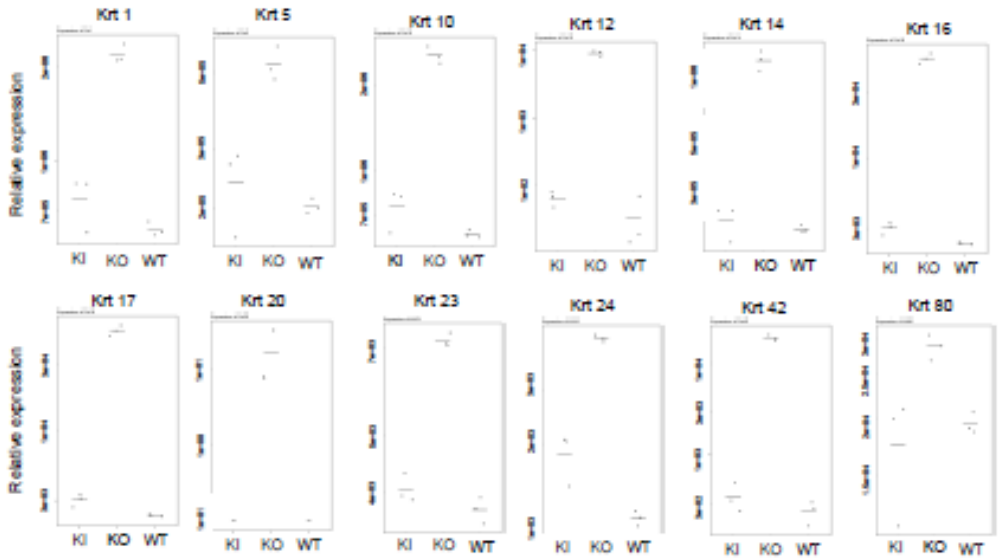

Figure 9. Comparison of mRNA levels of epidermal keratins among WT, KO, and KI rats.

Figure 10 lists the genes essential for keratinization and the formation of the cornified envelope that showed a marked increase in expression in KO compared to WT and KI (Suppl. Table S2). The protein encoded by Sprr1a is involved in epithelial protection and repair and is upregulated in

 doi:10.20944/preprints202411.1167.v1

response to inflammation and stress. Transglutaminases encoded by Tgm1 and Tgm3 are enzymes that crosslink proteins, strengthening the structure of the cornified layer, providing durability. TMEM79 (Transmembrane Protein 79) is a transmembrane protein associated with skin barrier function, particularly in skin protection, allergic reactions, and eczema. These genes are all related to enhancing the skin's barrier function. In KO rats, barrier function appears compromised, and their expression may have been induced to compensate.

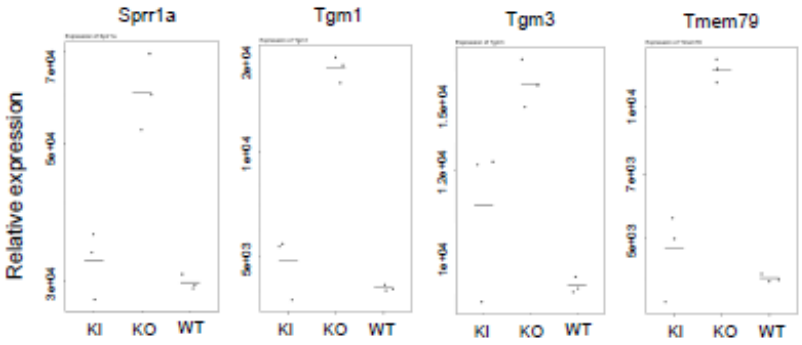

Figure 10. Comparison of mRNA levels of keratinization-related genes among WT, KO, and KI rats.

Figure 11 lists the keratins that were significantly reduced only in KO rats. The hair follicle comprises the hair shaft, inner root sheath, and outer root sheath. Among the keratins in Figure 9, Krt31, 32, 34–36, 39, 40, and 81–85 are present in the hair shaft and are collectively known as hair keratins. Krt25–28, 71, and 72 are keratins located in the inner root sheath [17]. The fact that these were significantly reduced in KO rats, and that hair loss and abnormal follicles were observed in KO rats, is in good agreement with the findings (Suppl. Table S2).

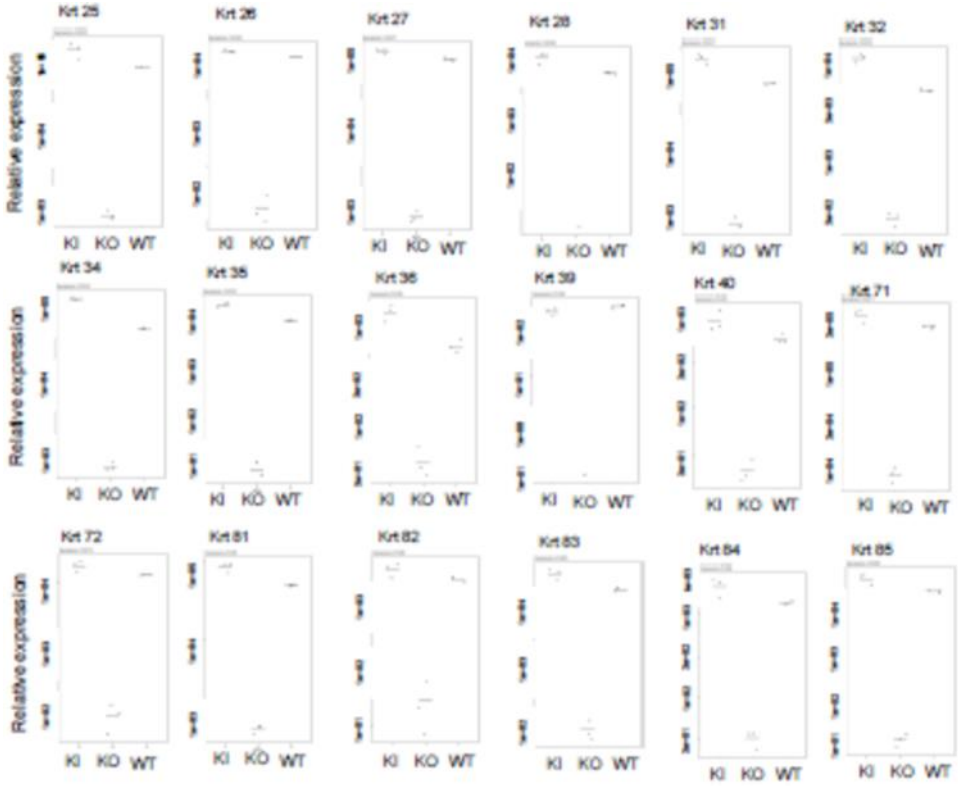

Figure 11. Comparison of mRNA levels of hair keratins and inner root sheath keratins among WT, KO, and KI rats.

 doi:10.20944/preprints202411.1167.v1

Figure 12 presents inflammation-related genes (IL1β, S100a8, S100a9) and a cell proliferation gene (Mki67) that showed increased expression only in KO. The skin of 30-week-old KO rats exhibits conditions reminiscent of symptoms seen in atopic dermatitis or psoriasis (Suppl. Figure 1), prompting an investigation of inflammation-related gene expression. IL-1β (interleukin-1 β) is a potent pro-inflammatory cytokine that plays a central role in immune response and inflammation. This protein is primarily produced by immune cells such as macrophages, neutrophils, and monocytes, and is released in response to stress signals from infection, trauma, or tissue damage. S100a proteins are calcium-binding proteins involved in cellular proliferation and differentiation. They are notably expressed in immune cells and are upregulated during inflammation to modulate immune response to infection and inflammation. Mki67 is an excellent marker for indicating cell proliferation as it is only expressed during cell division. In 30-week-old KO rats, a wavy skin structure is observed (Suppl. Figure 1), suggesting abnormal proliferation of keratinocytes. From these results, it is inferred that the skin of KO rats likely exhibits chronic inflammation and increased proliferation of epidermal keratinocytes.

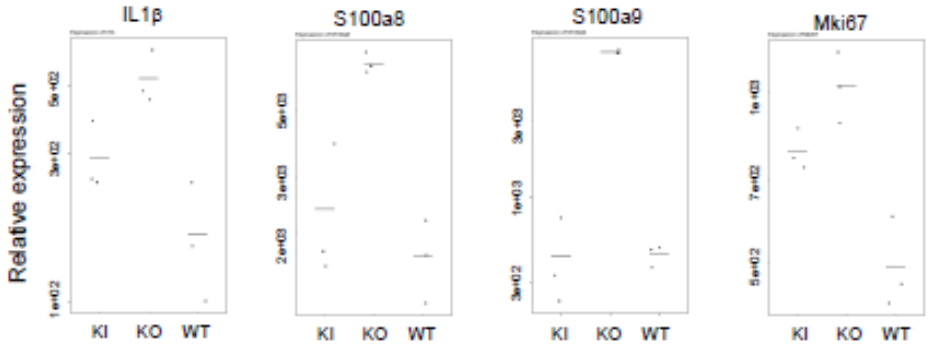

Figure 12. Comparison of mRNA levels of genes involved in inflammation (IL1β, S100a8. S100a9) or cell proliferation (Mki67) among WT, KO, and KI rats.

3. Discussion

Previous reports have shown that vitamin D has anti-inflammatory, anti-aging, and wound-healing properties in the skin [9,18,19]. However, it is unclear whether these effects are mediated through VDR or independent of VDR. In keratinocytes in the skin, vitamin D3 is synthesized from 7-dehydrocholesterol by sunlight exposure, and 25-hydroxylation by CYP2R1 and CYP27A1 in keratinocytes, followed by 1α-hydroxylation by CYP27B1, produces active vitamin D3 [20,21]. Furthermore, it is believed that both calcium and 1,25D3 synthesized in keratinocytes are necessary for keratinocyte differentiation and cornified envelope formation. Although CaSR, PLC, PKC, and AP-1 factor involvement have been suggested in this mechanism, the role of VDR remains uncertain. Meanwhile, Tian et al. [11] found that the administration of 1,25D3 was effective in wound repair and considered it an action of ligand-dependent VDR. On the other hand, based on the decreased expression of β-catenin signaling target genes such as Padi1, Dix, and Tubb3 in VDR-cKO mice, VDR is thought to form a complex with β-catenin and Lef1 to activate β-catenin signaling and promote keratinocyte proliferation [1]. This action of VDR is speculated to be ligand-independent. Furthermore, recent studies by Jokoh et al. [13] suggested that VDR plays an essential role in inducing keratinocyte apoptosis during the regression phase of the hair cycle. Thus, the mechanisms by which vitamin D and VDR affect keratinocyte metabolism, active vitamin D production, and keratinocyte proliferation, differentiation, and apoptosis are complex and remain unclear. We conducted this study to identify the most critical mechanisms among these actions.

One notable point of this study is the use of rats with VDR that do not bind ligands. VDR (R270L/H301Q) hardly binds to 1,25D3 and 25D3. We have confirmed that physiological concentrations do not cause nuclear translocation or induce CYP24A1 transcription. In the previous studies, mouse VDR (L304H) [22] and human VDR(L233S) [23] has been regarded as lacking ligand-binding ability so far. However, the affinity of mouse VDR(L304H) for 1,25D3 appears to be about

 doi:10.20944/preprints202411.1167.v1

1/10 of the WT-VDR. Similarly, studies using transgenic VDR-KO mice expressing human L233S specifically in keratinocytes appear to retain some extent of ligand-dependent VDR actions. In contrast, our rats differ significantly from the reported VDR mutants in that the double mutation of the two amino acid residues (Arg270 forms a hydrogen bond with the 1α-hydroxy group, and His301 forms a hydrogen bond with the 25-hydroxy group) contributing most to 1,25D3 binding results in the almost complete loss (less than 0.01%) of 1,25D3-dependent VDR function. It is noted that all enzymes required for synthesizing active vitamin D are present in keratinocytes [21], then the concentration of 1,25D3 might be higher in keratinocytes than in blood or other organs. To precisely differentiate between ligand-dependent and ligand-independent actions of VDR in keratinocytes, it is essential to use a VDR variant that completely lacks ligand-binding capability. VDR (R270L/H301Q) appears to be the most suitable candidate for this purpose. Comparing the skin of VDR (R270L/H301Q) rats with VDR-KO rats will highlight the ligand-independent actions of VDR in keratinocytes. To the best of our knowledge, the concentration of VDR ligands in the skin has not been previously reported. However, our RNA sequencing results demonstrated CYP24A1 expression in KO rats, while no expression was observed in both WT and KI rats (data not shown). This suggests that the concentration of VDR ligands in WT rat skin is exceedingly low. In addition, repression of CYP24A1 gene transcription by non-liganded VDR likely occurred in both WT and KI rats, as previously reported [24].

In HE staining, cyst formation was observed only in the 30-week-old KO rats, while KI rats were similar to WT rats. Western blot analysis showed a significant reduction in Krt14 in 4-week-old KO rats compared to WT and KI rats (Figure 3), consistent with the findings of Xie et al.'s qPCR analysis, which indicated reduced keratinization in 3-week-old VDR-KO mice [25]. No apparent skin abnormalities and normal hair growth were seen in 4-week-old KO rats. However, at 15 weeks, the amount of Krt14 protein was significantly higher than in WT and KI rats, and it was markedly elevated at 30 weeks. The levels of Krt1 and Krt5 proteins were also significantly increased in 30-week-old KO rats (Suppl. Fig). Consequently, RNA-seq was used to compare the gene expression among WT, KI, and KO rats. First, when examining the expression of genes essential for hair cycle regulations, their remarkable reduction was observed only in KO rats (Figure 8). Similarly, in 11-week-old VDR-KO mice [16], reductions in Shh, Lef1, Wnt10b, Bmp4, and Noggin were reported. In our current findings, a significant reduction was also observed in β-catenin gene expression, along with notable decreases in the Shh pathway (Shh) and the Wnt signaling pathway (Ctnnb1 (β-catenin), Lef1, Wnt10b). Conversely, Wise, an inhibitor of both the Wnt and Bmp signaling pathways, was increased in KO rats. Therefore, it can be inferred that the Wnt signaling pathway is markedly suppressed in KO rats. Additionally, Bmp4 was significantly decreased in the KO rats, while its inhibitor Noggin was also reduced. Considering the increase of Wise in KO rats, it is possible to assume that this pathway may also be downregulated in KO rats. No significant differences were observed between KI and WT rats in these pathways, indicating that ligand-independent VDR may play a crucial role in the expression of Shh, Wnt, and Bmp pathway-related genes.

The Hr mRNA level was higher in KO rats compared to WT and KI rats, which is consistent with the fact that Hr expression was higher in 11-week-old VDR-KO mice than in WT mice [16]."

Comparison of keratins expression among WT, KI, and KO rats revealed a remarkable decrease in KO rats in the expression of 18 types of hair keratin and the keratins specifically expressed in the inner root sheath [17,26]. These results are consistent with the absence of hair follicles in KO rats as shown in Figure 3. In contrast, the expression of 12 types of epidermal keratins was dramatically upregulated in KO rats, suggesting the enhanced proliferation of keratinocytes forming the epidermis layers (basal spinous, granular, and cornified). In addition, a proliferation of Krt10 positive cyst-forming keratinocytes [13] may be concerned. These findings are consistent with Western blot analysis (Krt14 in Figure 4, Krt1 and Krt5 in Suppl. Figure 2) and proteomic analysis (Krt24, and Krt80 in Suppl Table 3). Teichert et al. [16] also reported a reduction in the expression of 5 hair keratins and an increase in 2 epidermal keratins in VDR-KO mice. Additionally, KO rats showed a marked increase in gene expression related to keratinization and cornified envelope formation, essential for skin barrier function (Figure 6), consistent with proteomic analysis (Suppl Tables 4 and 5). Given the

 doi:10.20944/preprints202411.1167.v1

importance of the cornified envelope in skin barrier function, it is likely that KO rats exhibit enhanced skin barrier function. However, as shown in Figure 6, only KO rats exhibited a significant increase in trans-epidermal water loss (TEWL). Since an intact skin barrier would suppress water loss, the elevated TEWL suggests impaired skin barrier function in KO rats. The findings in Figure 12 also imply potential chronic inflammation in KO rat skin, with compromised barrier function possibly resulting from chronic inflammation. Therefore, the observed increase in keratinization and cornified envelope-related genes in KO rats may represent a compensatory mechanism for the decreased barrier function. Interestingly, even at 5 weeks, KO rats showed higher TEWL than WT and KI rats. However, HE staining revealed apparently normal skin with no signs of alopecia. Nonetheless, Western blot analysis of 4-week-old KO rats (Figure 5) suggested that keratinization may be insufficient, and the barrier function might be low. This finding appeared to be consistent with the lower keratinization of 3-week-old VDR-KO mice than WT-mice [27]. Although the TEWL values were high at 5, 10, and 30 weeks, we hypothesize that the underlying reasons differ between 5-week-old KO rats and 10- and 30-week-old rats.

Based on our current results and previous reports,

1. Non-liganded VDR is necessary for the expression of genes in Shh, Wnt, or BMP pathways essential for hair cycle regulations.
2. The initial hair cycle proceeds through anagen and catagen phases even in the absence of VDR.
3. The transition from catagen to telogen requires VDR-dependent apoptosis.of epithelial strand of hair follicle [13].
4. Epithelial strands of hair follicle that evade apoptosis form cysts, which continue to proliferate to result in the formation of wavy skin surfaces as cornified layers (Suppl. Figure 1).

Notably, in KO rats, there is a marked reduction in the key signaling pathways (Shh, Wnt, and Bmp), all of which play essential roles in the maintenance and differentiation of epidermal stem cells, hair follicle formation, regeneration, and wound healing. Furthermore, the Wnt, Shh, and BMP pathways interact with each other (cross-talk) to regulate complex physiological processes. Therefore, KO rats likely experience a disorderly state where these regulatory processes are significantly less functional. It is noteworthy that the non-liganded VDR regulates the transcription of these crucial genes.

It is known that Hairless (Hr) forms a complex with non-liganded VDR and binds to VDRE, suppressing gene expression [28]. However, we hypothesize that non-liganded VDR might have a mechanism promoting transcription of Shh, Ctnnb1, Lef1, Wnt10b, and Bmp4 genes. This is quite essential function of VDR, and we aim to investigate this further.

4. Materials and Methods

4.1. Animals and Diets

Jcl:Wistar rats were obtained from CLEA Japan Inc. (Tokyo, Japan). Embryonic microinjection for genome editing was performed by KAC Co., Ltd. (Kyoto, Japan). All of rats were kept at room temperature (22 to 26 ˚C), and in 50 to 55% humidity with a 12 h light/dark cycle. They were allowed food and water ad libitum and fed CE-2 (Oriental Yeast Co., Tokyo, Japan). Homozygotes of KO rats were maintained by mating of homozygotes. Genotype was determined by electrophoresis of PCR products of the target site for KO rats. All of experiment were conducted with male rats. All experimental protocols using animals were performed in accordance with the Guidelines for Animal Experiments at Toyama Prefectural University and were approved by the Animal Research and Ethics Committee of Toyama Prefectural University.

4.2. Immunofluorescence

Each rat skin sample was fixed with 4% PFA (FUJIFILM Wako Pure Chemical Corporation, Tokyo, Japan) for 15 h at 4℃. The fixed samples were mounted with O.T.C compound (Sakura Finetek Japan, Tokyo, Japan) in a container and feezed in liquid nitrogen. The frozen sections were prepared with cryostat microtome (Leica, Tokyo, Japan) thickness 20μm each sample, and sticked it to glass

 doi:10.20944/preprints202411.1167.v1

slaids. Anti-VDR antibody (D2K6W) Rabbit mAb (Cell Signaling Technology, Danvers, MA, USA), and Alexa Flour 488 goat anti-rabbit IgG (Invitrogen,Carlsbad, USA) were used for immunofluorescence [29]. After staining nuclei with DAPI, samples were observed using phase contrast microscopy (Olympus, Tokyo Japan).

Table 1. Antibodies used in Western blot analysis.

Protein	First Ig	Second Ig
VDR	Anti-VDR antibody (D2K6W) Rabbit mAb (Cell Signaling Technology)	Alexa Flour 488 goat anti-rabbit IgG (Invitrogen)
Krt14	Anti-Cytokeratin 14 polyclonal rabbit Ig (Proteintech Group, Inc.)	HRP-conjugated goat anti-rabbit #7074 (Cell Signaling Technology)
Krt1, 5, and 8	clone PCK-26, purified from hybridoma cell culture C5992 (Sigma-Aldrich)	HRP-conjugated horse anti-mouse IgG(H+L) #7076 (Cell Signaling Technology)
b-actin	◎-Actin Antibody #4967 (Cell Signaling Technology)	HRP-conjugated Anti-rabbit #7074(Cell Signaling Technology)

4.3. HE Staining

Each rat skin sample was fixed with 4% PFA (FUJIFILM Wako Pure Chemical Corporation, Osaka, Japan) for 15h at 4℃. The fixed samples were mounted with O.T.C compound (Sakura Finetek, Japan) in container and feezed in liquid nitrogen. Frozen sections were obtained by cryostat microtome (Leica, Tokyo, Japan) with thickness of 20-25μm, and stuck to glass slides [7]. The 4% PFA solution was dripped to the sample glass, which was incubated at room temperature for 10 min, and washed with water for 10 min. Hematoxylin was dripped on the sample glass, which was incubated at room temperature for 15min, and washed with water for 10min. Eosin-alcohol were dripped on the sample glass, which was incubated at room temperature for 2min, and washed with water for 2 min, 70 % EtOH for 2min, 80% EtOH for 2min, 90% EtOH for 2min, 100% EtOH for 2min, and then washed with xylene twice. The resultant HE stained samples were observed using a phase contrast microscopy (Olympus, Tokyo Japan).

4.4. Western Blot Analysis

Rats back hair was shaved with hair clipper and cut out with scissors, and then homogenized with Minylis personal homogenizer (bertin technologies, Montigny-le-Bretonneux, France). The resultant tissue lysate containing 20 μg protein was applied to each lane of the gel, and then subjected to SDS–PAGE on 4 to 20% linear gradient polyacryl amide/SDS gels. Molecular size maker (blue pre-stained protein Standard, Broad Range P7718S, New England BioLabs. Inc., Ipswich, MA, USA) was loaded with 3 μl. After electrophoresis, gels were electrotransferred onto PVDF membranes. The membranes were incubated in TBS-T containing 5% skim milk, and then incubated with 1st antibody (table). The membranes were washed three times with Tris-buffered saline containing 0.05% Tween 20 (TBS-T) and incubated with horseradish peroxidase-conjugated goat anti-rabbit IgG (Cell Signaling Technology, Danvers, MA, USA). The membranes were washed with Tris-buffered saline containing 0.05% Tween 20 (TBS-T), and then followed by enhanced chemiluminescence immunodetection method (Amersham Pharmacia Biotech, Buckinghamshire, England).

4.5. Measurement of Moisture Transpiration (TEWL)

Rats back hair were shaved with hair clipper and TEWL was detecteted with VAPOSCAN AS-VT100 (Asch Japan Co.,Ltd., Tokyo, Japan).The TEWL is calculated as the amount of water vapor flux per unit area of skin (usually expressed in g/m²/h). This is based on the following formula derived from Fick's Law:

$TEWL=D\times dC/dx$

 doi:10.20944/preprints202411.1167.v1

D is the diffusion coefficient of water vapor in air. dC/dx is the concentration gradient of water vapor measured by the sensors [14].

4.6. RNA-Seq Analysis

The back hairs of the 30 weeks-old male rats (WT, KO and KI groups, with 3 rats in each group) were shaved with hair clipper and skin were cut with sizzlers. The collected skins were rapidly freezed with liquid nitrogen, and grinded into powder with a sandpaper. Total RNA was extracted with ISOGEN II (NIPPON GENE CO., LTD, Toyama, Japan). The preparation of a cDNA library and sequencing was conducted at Rhelixa Co., Ltd (Tokyo, Japan) with Illumina Nova Seq 6000. RNA-Seq reads generated from these 9 libraries were adapter-trimmed using Trim Galore! (ver. 0.6.10) [30] and cutadapt (ver. 4.4) [31] The cleaned reads were subsequently mapped to the R. norvegicus genome assembly (Rnor_6.0 [32]) using HISAT2 (ver. 2.1.0) [33] with default parameters. Gene expression quantification was performed using StringTie (ver. 2.2.1) [34] and prepDE.py (http://ccb.jhu.edu/software/stringtie/dl/prepDE.py) with a GTF file (Rattus_norvegicus.Rnor_6.0.104 [32]) were used to generate the count matrix. The count data were normalized by the trimmed mean of M values (TMM) method provided in the TCC library (ver. 1.42.0) [35,36]. To cluster genes based on similar expression patterns, hierarchical clustering analysis was conducted using the edgeR library (ver. 4.0.16) based on the normalized count data [37]. To identify differentially expressed genes (DEGs) between samples (WT vs KO, WT vs KI and KO vs KI), we used the TCC package, with default options, in which the TMM method and edgeR-based DEG analysis were employed. A Venn diagram was generated to illustrate the significant DEGs (FDR < 0.05) shared between WT vs KO and WT vs KI comparisons, utilizing the VennDiagram package (ver. 1.7.3) [38]. Additionally, the normalized count data were used to compare the gene expression levels between WT, KI, and KO rats, which were visualized in dot plots.

4.7. Statistical Analysis

The statistical significance of differences in Figs. 8 and 12 was analyzed by the Student's t-test. *: $p<0.05$, **:$p<0.01$, ***: $p<0.001$, n.s.: not significant (Suppl. Table S1). The statistical significance of differences in Figs. 9 and 11 was analyzed by Tukey-Kramer procedure with one-way ANOVA.*: $p<0.05$, **:$p<0.01$, ***: $p<0.001$, n.s.: not significant (Suppl. Table S2)

5. Conclusions

Comparison of WT, VDR-KO, and our novel KI rats, which have VDR completely lacking ligand-binding ability, clearly demonstrated that "non-liganded VDR plays a critical role in the differentiation, proliferation, and apoptosis of keratinocytes in both hair follicles and the epidermis.

Supplementary Materials: The following supporting information can be downloaded at: www.mdpi.com/xxx/s1, Figure S1-4: Table S1-5.

Author Contributions: Conceptualization, S.Kise, T.S., and K..Y; methodology, S.Kise. S.M and T.S..; software, S. Kise, and S. M.; validation, S. Kise, T.S, and K.Y.; formal analysis,S. Kise and S.M. ; investigation, S. Kise, S. M. and T.S. resources, S. M.; data curation, T.S. H.K., S. Kinuya. and K.Y.; writing—original draft preparation, S. Kise and T. S..; writing—review and editing, H.K., S. Kinuya., and K.Y.; visualization, S. Kise, S.M., and T.S.; supervision, H.K., S. Kinuya.; project administration, T.S., S. Kinuya, and K.Y; funding acquisition, T.S. All authors have read and agreed to the published version of the manuscript.".

Funding: This work was supported by Grants-in-Aid from the Japan Society for the Promotion of Science (22H02263).

Institutional Review Board Statement: I All experimental protocols using animals were performed in accordance with the Guidelines for Animal Experiments at Toyama Prefectural University and were approved by the Animal Research and Ethics Committee of Toyama Prefectural University. (protocol code XXX and date of approval)." for studies involving animals.

 doi:10.20944/preprints202411.1167.v1

Data Availability Statement: The datasets generated or analyzed during the current study are avail-able from the corresponding author (T.S.) on reasonable request. A genomic sequence of Vdr gene of Vdr KO rats containing the mutated position is available in DDBJ data base accession number 370 LC764592 (http://getentry.ddbj.nig.ac.jp/top-j.html).

Acknowledgments: This work was supported by JST SPRING, Grant Number JPMJSP2135.

Conflicts of Interest: The authors declare no conflicts of interest.

References

1. Bouillon R, Carmeliet G, Verlinden L, van Etten E, Verstuyf A, Luderer HF, Lieben L, Mathieu C, Demay M. Vitamin D and human health: lessons from vitamin D receptor null mice. Endocr Rev. 29, 726-776 (2008)
2. Cui X, Gooch H, Petty A, McGrath JJ, Eyles D. Vitamin D and the brain: Genomic and non-genomic actions. Mol Cell Endocrinol. 453, 131-143 (2017)
3. Tohda C, Urano T, Umezaki M, Nemere I, Kuboyama T. Diosgenin is an exogenous activator of 1,25D_3-MARRS/Pdia3/ERp57 and improves Alzheimer's disease pathologies in 5XFAD mice. Sci Rep. 2, 535 (2012)
4. Yahyavi SK, Boisen IM, Cui Z, Jorsal MJ, Kooij I, Holt R, Juul A, Blomberg Jensen M. Calcium and vitamin D homoeostasis in male fertility. Proc Nutr Soc. 83, 95-108 (2024)
5. Malloy PJ, Feldman D. The role of vitamin D receptor mutations in the development of alopecia. Mol Cell Endocrinol. 347, 90-96 (2011)
6. Kise S, Iijima A, Nagao C, Okada T, Mano H, Nishikawa M, Ikushiro S, Kanemoto Y, Kato S, Nakanishi T, Sato S, Yasuda K, Sakaki T. Functional analysis of vitamin D receptor (VDR) using adenovirus vector. J Steroid Biochem Mol Biol. 230, 106275 (2023).
7. Nishikawa M, Yasuda K, Takamatsu M, Abe K, Okamoto K, Horibe K, Mano H, Nakagawa K, Tsugawa N, Hirota Y, Horie T, Hinoi E, Okano T, Ikushiro S, Sakaki T. Generation of novel genetically modified rats to reveal the molecular mechanisms of vitamin D actions. Sci Rep. 10, 5677 (2020)
8. Iwai Y, Iijima A, Kise S, Nagao C, Senda Y, Yabu K, Mano H, Nishikawa M, Ikushiro S, Yasuda K, Sakaki T. Characterization of Rickets Type II Model Rats to Reveal Functions of Vitamin D and Vitamin D Receptor. Biomolecules. 13, 1666 (2023).
9. Oda Y, Tu CL, Menendez A, Nguyen T, Bikle DD. Vitamin D and calcium regulation of epidermal wound healing. J Steroid Biochem Mol Biol. 164, 379-385 (2016)
10. Pálmer HG, Martinez D, Carmeliet G, Watt FM. The vitamin D receptor is required for mouse hair cycle progression but not for maintenance of the epidermal stem cell compartment. J Invest Dermatol. 128, 2113-2117 (2008)
11. Tian XQ, Chen TC, Holick MF. 1,25-dihydroxyvitamin D3: a novel agent for enhancing wound healing. J Cell Biochem. 59, 53-56 (1995)
12. Bikle DD, Ng D, Tu CL, Oda Y, Xie Z. Calcium- and vitamin D-regulated keratinocyte differentiation. Mol Cell Endocrinol. 177,161-171 (2001)
13. Joko Y, Yamamoto Y, Kato S, Takemoto T, Abe M, Matsumoto T, Fukumoto S, Sawatsubashi S. VDR is an essential regulator of hair follicle regression through the progression of cell death. Life Sci Alliance. 2023 Sep 6;6(11):e202302014.
14. Schwindt DA, Wilhelm KP, Maibach HI. Water diffusion characteristics of human stratum corneum at different anatomical sites in vivo. J Invest Dermatol. 111, 385-389 (1998)
15. Hsieh JC, Estess RC, Kaneko I, Whitfield GK, Jurutka PW, Haussler MR. Vitamin D receptor-mediated control of Soggy, Wise, and Hairless gene expression in keratinocytes. J Endocrinol. 220, 165-178 (2014)
16. Teichert A, Elalieh H, Bikle D. Disruption of the hedgehog signaling pathway contributes to the hair follicle cycling deficiency in Vdr knockout mice. J Cell Physiol. 225, 482-489 (2010)
17. Kalabusheva EP, Shtompel AS, Rippa AL, Ulianov SV, Razin SV, Vorotelyak EA. A Kaleidoscope of Keratin Gene Expression and the Mosaic of Its Regulatory Mechanisms. Int J Mol Sci. 24, 5603 (2023)
18. Halioua B, Caillet G, Taieb C, Bewley A, Snel-Prentø A, Praestegaard M, Armstrong A, Pinter A. A novel calcipotriol and betamethasone dipropionate (CAL/BDP) PAD-cream demonstrates greater improvements in daily activities and personal relationships than CAL/BDP gel/TS: A post-hoc analysis of DLQI outcomes from two phase 3 placebo-controlled randomized clinical trials in mild-to-moderate psoriasis. J Eur Acad Dermatol Venereol. 38, e326-e328 (2024)
19. Sayegh S, Fantecelle CH, Laphanuwat P, Subramanian P, Rustin MHA, Gomes DCO, Akbar AN, Chambers ES. Vitamin D3 inhibits p38 MAPK and senescence-associated inflammatory mediator secretion by senescent fibroblasts that impacts immune responses during ageing. Aging Cell. 23, e14093 (2024).
20. Bikle DD, Nemanic MK, Whitney JO, Elias PW. Neonatal human foreskin keratinocytes produce 1,25-dihydroxyvitamin D3. Biochemistry. 25, 1545-1548 (1986)
21. Bikle DD. Vitamin D: Production, Metabolism and Mechanisms of Action. 2021 In: Feingold KR, Anawalt B, Blackman MR, Boyce A, Chrousos G, Corpas E, de Herder WW, Dhatariya K, Dungan K, Hofland J, Kalra

S, Kaltsas G, Kapoor N, Koch C, Kopp P, Korbonits M, Kovacs CS, Kuohung W, Laferrère B, Levy M, McGee EA, McLachlan R, New M, Purnell J, Sahay R, Shah AS, Singer F, Sperling MA, Stratakis CA, Trence DL, Wilson DP, editors. Endotext [Internet]. South Dartmouth (MA): MDText.com, Inc.; 2000–. PMID: 25905172.

22. Huet T, Laverny G, Ciesielski F, Molnár F, Ramamoorthy TG, Belorusova AY, Antony P, Potier N, Metzger D, Moras D, Rochel N. A vitamin D receptor selectively activated by gemini analogs reveals ligand dependent and independent effects. Cell Rep. 10, 516-526 (2015)
23. Skorija K, Cox M, Sisk JM, Dowd DR, MacDonald PN, Thompson CC, Demay MB. Ligand-independent actions of the vitamin D receptor maintain hair follicle homeostasis. Mol Endocrinol. 19, 855-862 (2005)
24. Alimirah F, Vaishnav A, McCormick M, Echchgadda I, Chatterjee B, Mehta RG, Peng X. Functionality of unliganded VDR in breast cancer cells: repressive action on CYP24 basal transcription. Mol Cell Biochem. 342, 143-150 (2010)
25. Xie Z, Komuves L, Yu QC, Elalieh H, Ng DC, Leary C, Chang S, Crumrine D, Yoshizawa T, Kato S, Bikle DD. Lack of the vitamin D receptor is associated with reduced epidermal differentiation and hair follicle growth. J Invest Dermatol. 118, 11-16 (2006)
26. Hesse M, Zimek A, Weber K, Magin TM. Comprehensive analysis of keratin gene clusters in humans and rodents. Eur J Cell Biol. 83, 19-26 (2004)
27. Xie Z, Komuves L, Yu QC, Elalieh H, Ng DC, Leary C, Chang S, Crumrine D, Yoshizawa T, Kato S, Bikle DD. Lack of the vitamin D receptor is associated with reduced epidermal differentiation and hair follicle growth. J Invest Dermatol. 118, 11-16 (2002)
28. Xie Z, Chang S, Oda Y, Bikle DD. Hairless suppresses vitamin D receptor transactivation in human keratinocytes. Endocrinology 147, 314-323 (2006)
29. Kise S, Iijima A, Nagao C, Okada T, Nishikawa M, Ikushiro S, Nakanishi T, Sato S, Yasuda K, Sakaki T. Gene therapy for alopecia in type II rickets model rats using vitamin D receptor-expressing adenovirus vector. Sci Rep. 13, 18528 (2023)
30. Krueger, F. Trim Galore (RRID: SCR_011847). https://github.com/FelixKrueger/TrimGalore. (2015).
31. Martin, M. Cutadapt removes adapter sequences from high-throughput sequencing reads. EMBnet.journal 17, 10–12 (2011).
32. Ramdas S, Ozel AB, Treutelaar MK, et al.: Extended Regions of Suspected Mis-Assembly in the Rat Reference Genome. Sci Data. 2019; 6(1): 39.
33. Kim, D., Langmead, B. & Salzberg, S. L. HISAT: a fast spliced aligner with low memory requirements. Nat. Methods 12, 357–360 (2015).
34. Pertea, M. et al. StringTie enables improved reconstruction of a transcriptome from RNA-seq reads. Nat. Biotechnol. 33, 290–295 (2015).
35. Robinson, M. D. & Oshlack, A. A scaling normalization method for differential expression analysis of RNA-seq data. Genome Biol. 11, R25 (2010).
36. Sun, J., Nishiyama, T., Shimizu, K. & Kadota, K. TCC: an R package for comparing tag count data with robust normalization strategies. BMC Bioinformatics 14, 219 (2013).
37. Robinson, M. D., McCarthy, D. J. & Smyth, G. K. edgeR: a Bioconductor package for differential expression analysis of digital gene expression data. Bioinformatics 26, 139–140 (2010).
38. Chen, H., Boutros P. C. VennDiagram: a package for the generation of highly-customizable Venn and Euler diagrams in R. BMC Bioinformatics 12, 35 (2011).
39. Hara Y, Kawasaki N, Hirano K, Hashimoto Y, Adachi J, Watanabe S, Tomonaga T. Quantitative proteomic analysis of cultured skin fibroblast cells derived from patients with triglyceride deposit cardiomyovasculopathy. Orphanet J Rare Dis. 8, 197 (2013)